ACS Partner Journal

Journal of the American Society for Mass Spectrometry

pubs.acs.org/jasms

Article

Statistical Analysis of Photon-Activated Chimeric Tandem Mass Spectra

Published as part of Journal of the American Society for Mass Spectrometry special issue "Fenn: Photoactivation and Ion Activation".

Félix Truong, Laurent Nahon, and Alexandre Giuliani*

Cite This: *J. Am. Soc. Mass Spectrom.* 2026, 37, 649−656

Read Online

ACCESS | Metrics & More | Article Recommendations | Supporting Information

ABSTRACT: Photon activation is a powerful means of inducing controlled fragmentation in mass spectrometry, but the simultaneous activation of multiple precursor ions may produce multiplexed tandem mass spectra that are difficult to interpret. In this work, we show that such photon-activated multiple precursor spectra can be decomposed into individual precursor contributions using correlation-based and information-theoretic approaches. We propose a general, data-driven framework for the statistical resolution of multiplexed photon-activated MS/MS spectra based on the statistical treatment of the spectra followed by clustering analysis. This approach allows statistical tandem mass spectra to be obtained without prior knowledge of the precursor identities.

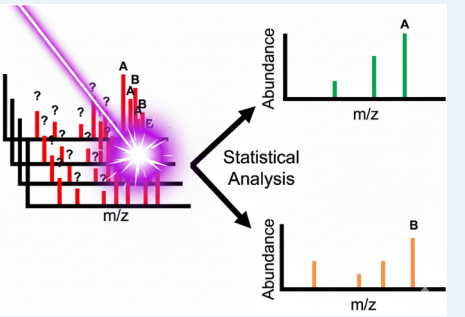

INTRODUCTION

Photon activation has gained significant interest over the past decade in tandem mass spectrometry applications. The UV photon energy range is widely used for photodissociation, particularly in bioanalysis.[1−3] While lasers are typically employed, other sources, such as discharge lamps[4,5] or synchrotron radiation in the VUV[6,7] or in the X-ray domain,[8] have also been employed. Optimizing photon activation conditions, such as wavelength selection, irradiation duration, and the photon source flux, is critical to control the extent of multiphoton absorption and ensure single-photon absorption, which is critical for ion spectroscopy. Developing data processing methods to identify the origins of fragments and derive precise product and precursor abundances is essential.

The principle of covariance mapping, developed by Frasinski and collaborators in the 1990s,[9] has been initially applied to study the Coulomb explosion of molecules. In this approach, a small variation of ion signals measured within a series of data acquisitions reveals the relationship between these variables. The covariance mapping has found applications in several fields,[10] including notably analytical mass spectrometry (MS)[11−13] with the application of partial covariance mapping to tandem MS. In such a case, the total ion current (TIC) serves as a partial variable to remove the TIC-related intensity fluctuations.[11] The resulting maps reveal relationships between complementary fragments.[14] Partial covariance has been applied to the top-down analysis of model proteins using low-resolution machines.[12] The reliability of correlation scores was evaluated by using normalized metrics based on covariance. While covariance mapping appears promising for proteomic analysis, most applications have focused on single precursors, except in the case involving isobaric species. Recently, statistical scoring through mutual information and Pearson correlation[15] or covariance[16] analysis has been extended to the separation of distinct precursors activated simultaneously.

This work presents the application of Pearson correlation to the photoionization of a mixture of two peptides and of conditional mutual information to a mixture of three small proteins. In addition, we show that using hierarchical clustering methods, extracted tandem mass spectra can be obtained without any prior knowledge of the sample composition.

EXPERIMENTAL SECTION

Photon Activation Setup

Experiments were conducted using a modified LTQ-XL ion trap[17] coupled to the DESIRS beamline at the SOLEIL synchrotron radiation facility.[18] Briefly, the LTQ was adapted to allow VUV irradiation of the ions stored in the trap. A beam shutter placed upstream of the ion trap controlled the irradiation time. The photon energy was selected using the normal-incidence monochromator of the beamline covering the 5−40 eV range. Here, the ions were selected by a 100 Th isolation window centered on the average m/z

Received: October 29, 2025
Revised: January 22, 2026
Accepted: January 29, 2026
Published: February 11, 2026

ratio of the precursor of interest and activated by monochromatic VUV photons of 16 eV (77.56 nm) and 20 eV (62.04 nm) following a regular tandem mass spectrometry scheme. Irradiation times ranged from 350 to 500 ms. Each photon activation mass spectrum was recorded, and the acquisition was carried out until 5000 to 10000 individual tandem mass spectra were measured.

Samples

All samples (W8-Substance P, Melittin, Lysozyme, Cytochrome C, Ubiquitin, and methanol) were obtained from Sigma-Aldrich and used without further purification. The samples were dissolved in a 50% water−methanol solution at a concentration of 10 μM and infused at 5 μL/min in the electrospray source.

DATA PROCESSING

A schematic workflow of the data processing methods is presented in Figure 1. The different steps are discussed below.

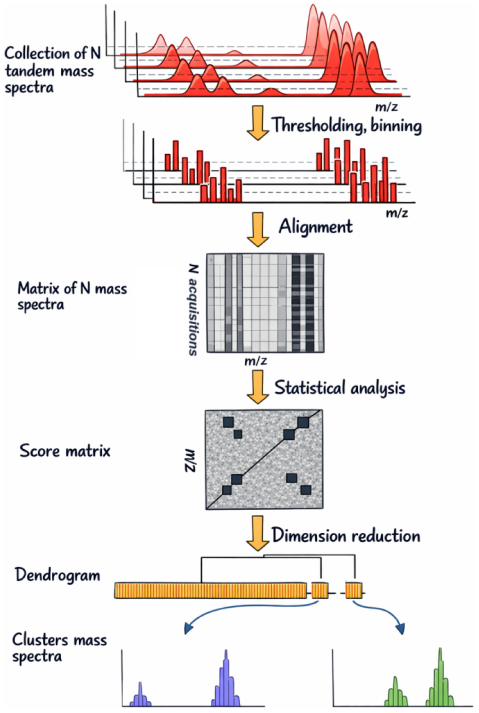

Figure 1. Schematic data processing workflow showing the different stages from the data collection to the construction of mass spectra associated with the clusters found after dimension reduction.

Data Reduction and Integration

For each experiment, mass spectra were recorded continuously during irradiation. Individual spectra were aligned and averaged to generate the reference mean spectrum. To create the temporal series of ion abundances, intensities below 1% of the base peak were first excluded. This process is referred to as thresholding in Figure 1. Then, ion abundances were extracted over defined m/z intervals, which is depicted as binning in Figure 1. The m/z axis is divided into discrete bins of 1 Th for the peptide mixture and 3 Th for the protein mixtures, resulting in 1069 and 275 variables, respectively. For each variable, the abundance is extracted, leading to a matrix for which the columns represent the mass spectrometric variables and the rows represent the acquisition number. All the processing steps were performed using the Julia language[19] and the MassJ package.[20]

Partial Covariance and Correlation Mapping

Partial Pearson correlations were computed between ion intensities (statistical analysis in Figure 1) using the total ion current (TIC) as a control variable to remove common intensity fluctuations using the StatsBase Julia package. The resulting symmetric correlation maps highlight positive correlations (ions varying together, usually from the same precursor) and negative correlations (anticorrelated ions from different precursors). These maps were visualized as 2D heatmaps, where diagonal blocks correspond to the self-correlation of isotopic distribution and off-diagonal regions reveal cross-correlations between fragments.

Information-Theoretic Analysis

In order to address the limitations of linear correlation, conditional mutual information (CMI) was introduced as a nonlinear metric (statistical analysis in Figure 1). Calculations were performed using the EntropyInvariant package.[21] CMI quantifies the shared information between two ion signals after conditioning on a third variable (the TIC). This method produces exclusively positive scores that facilitate the interpretation of relationships between fragments, even in complex cases where linear correlations are ambiguous. By capturing nonlinear dependencies, CMI improves robustness in multiprotein mixtures with overlapping ions, where fragments may have ambiguous or unknown origins, making their assignment to the correct precursors difficult. Conditioning on a third variable removes confounding effects and highlights the true statistical dependencies between the ions.

Dimensionality Reduction and Clustering

Hierarchical agglomerative clustering (Ward method) was applied to the correlation matrices to group ions according to their statistical relationships. Agglomerative clustering, labeled as dimensionality reduction in Figure 1, starts with individual variables as an individual cluster and repeatedly merges the two closest clusters. The optimal number of clusters was determined using the "elbow" method[22] based on the intracluster sum of squares (WSS), which identifies in our case the point beyond which additional clusters provide diminishing improvement in cluster compactness.

RESULTS AND DISCUSSION

Two-Precursor Mixture

Simultaneous photon activation of the W8-Substance P singly protonated ion and the Melittin doubly protonated ion at 16 eV produced a multiplexed tandem mass spectrum containing fragment ions from both peptides. The photon energy is sufficient to ionize the protonated peptide ions.[6,23] Although the ionization energy of the singly protonated ion of Substance P has been reported at 10.3 ± 0.1 eV[23] by photoionization action spectroscopy, the ionization energy of the doubly protonated ion of Melittin remains unknown. The only ionization energy data available concern the singly protonated ion at 10.6 ± 0.4 eV and higher Melittin charge states both measured by electron impact ionization.[24,25] The same method yielded a value of 10.7 ± 0.5 eV for Substance P. The ionization energy of the doubly protonated ion of Substance P was found to be 12.2 ± 0.7 eV by electron impact and 11.7 ± 0.1 eV by photon impact. Based on these values, the ionization energy of the $[M+2H]^{2+}$ Melittin ion is expected to be slightly below 12 eV.

https://doi.org/10.1021/jasms.5c00358
J. Am. Soc. Mass Spectrom. 2026, 37, 649−656

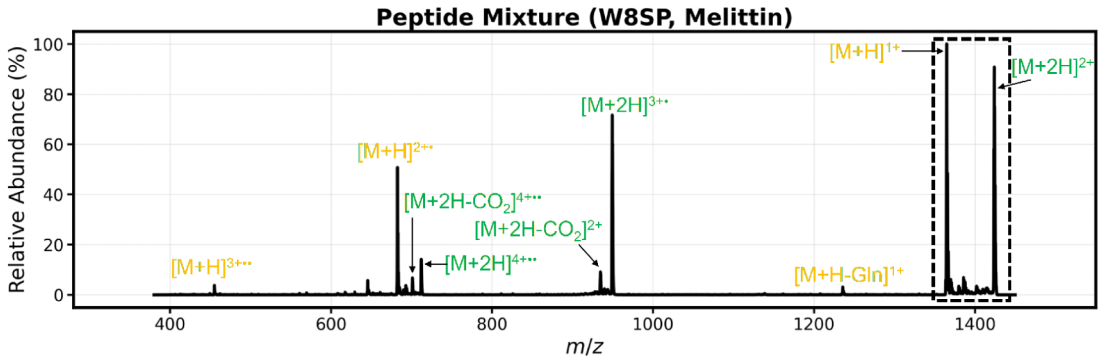

Figure 2. Average mass spectrum after 16 eV irradiation of a mixture of singly protonated W8-Substance P (W8SP) and the doubly protonated Melittin ions. The box indicates the selection region. The yellow labels refer to Substance P and the green ones to Melittin.

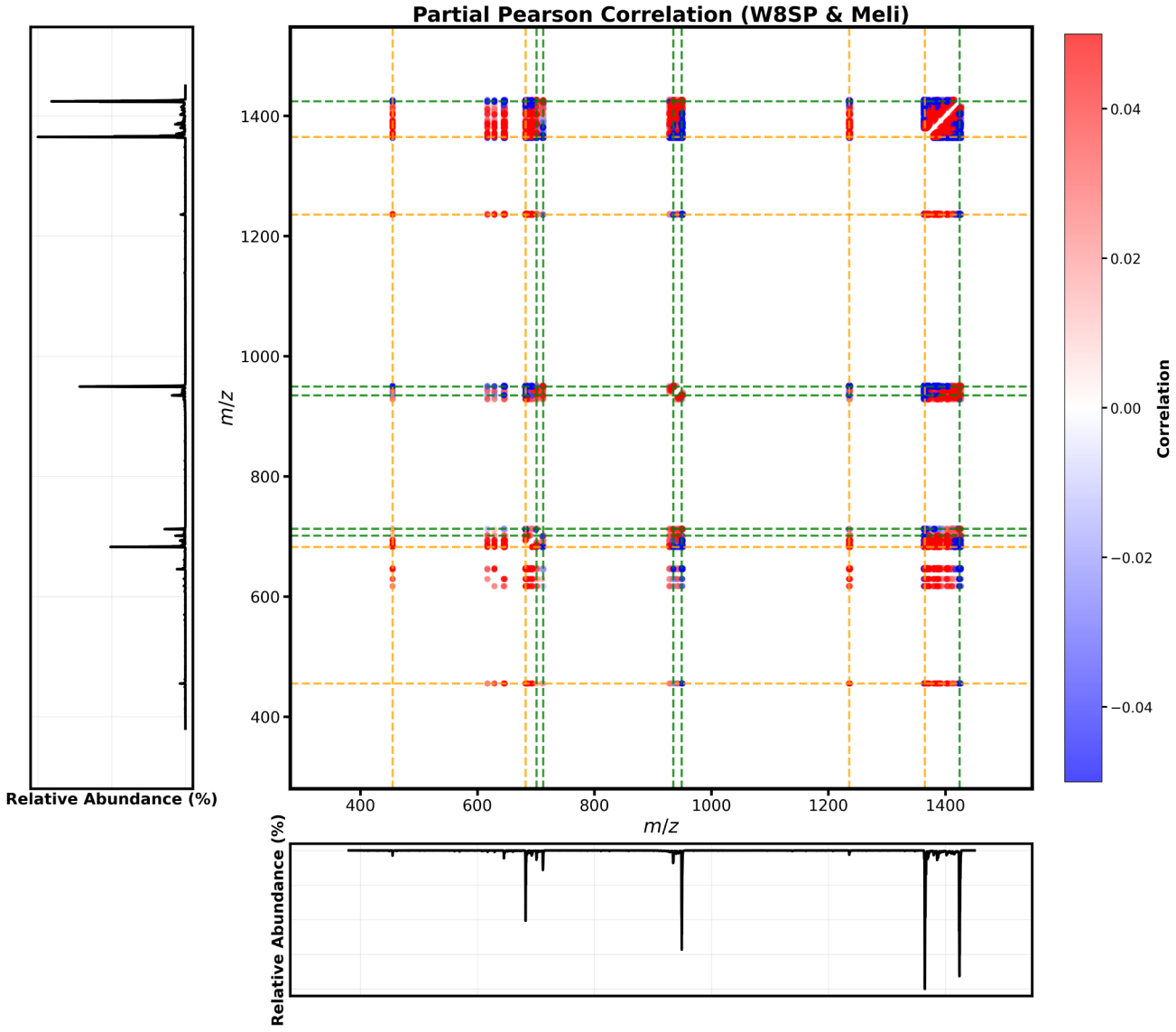

Figure 3. Partial Pearson correlation maps for Substance P and Melittin photon activation. The average mass spectrum (Figure 2) is presented at the bottom and on the left-hand side of the map. The colored dotted lines connect the features belonging to the same groups for Substance P (yellow) and Melittin (green).

Figure 2 presents the product ion mass spectrum after irradiation of m/z 1400, allowing both ions to be selected and activated simultaneously. The yellow labels in Figure 2 refer to Substance P and the green ones to Melittin.

Both peptide ions produce mainly ionization products along with minor abundance fragment ions coming from neutral losses. The irradiation time of 500 ms is long enough to allow product ions to absorb photons and thus leads to consecutive

https://doi.org/10.1021/jasms.5c00358
J. Am. Soc. Mass Spectrom. 2026, 37, 649−656

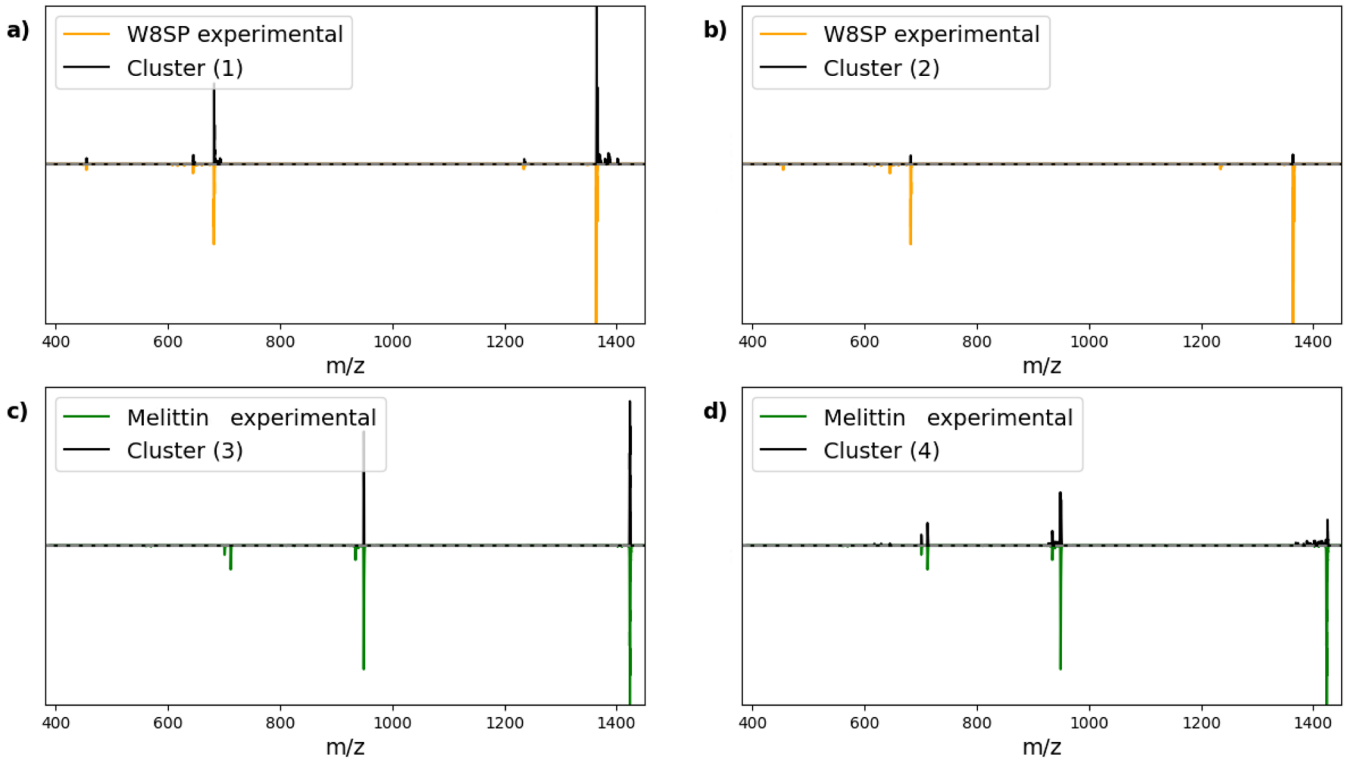

Figure 4. Comparison of the mass spectra of clusters 1 to 4 with experimental photon activation of the individual precursors. (a) Cluster 1 and W8-Substance P $[M + H]^+$ ion. (b) Cluster 2 and W8-Substance P $[M + H]^+$ ion. (c) Cluster 3 and Melittin $[M+2H]^{2+}$ ion. (d) Cluster 4 and Melittin $[M+2H]^{2+}$ ion.

multiple ionization. Hence, we observe the W8SP ions $[M + H]^{2+\bullet}$ via single photoionization along with the $[M + H]^{3+\bullet\bullet}$. For Melittin, we observe $[M+2H]^{3+\bullet}$ from the photoionization of the precursor along with $[M+2H]^{4+\bullet\bullet}$ and neutral losses. Approximately 5500 acquisitions were recorded. Figure S1 presents the relative abundances of both precursor ions. The variables extracted from the mass spectrometric acquisition are denoted as $X = X_i$ for $i = 1,\cdots,N$, where N is the number of acquisitions. The total ion current (TIC) was calculated as $I = \sum_i X_i$. Partial Pearson correlations ($r_{XX\cdot I}$) were computed between ion signals, with the TIC (I) as the partial variable:

$$r_{XY\cdot I} = \frac{r_{XY} - r_{XI}r_{YI}}{\sqrt{(1 - r_{XI}^2)(1 - r_{YI}^2)}} \quad (1)$$

The Y variable represents the transpose of the X array of data.[10]

Figure 3 shows the partial Pearson correlation map with the average mass spectrum of Figure 2 on the sides and the bottom. Diagonal blocks represent self-correlation (equal to 1) and have been removed for readability. The blue and red colors indicate anticorrelated (negative values) and correlated signals (positive values), respectively. Distinct groups of signals appearing anticorrelated correspond to the two precursors. In particular, the W8-Substance P precursor is found at m/z = 1364.83. This ion presents, either vertically or horizontally (owing to the symmetry of the map), connections in red with features at m/z 1235.66, 682.41, and 455, which correspond to neutral loss ions and to the photoionization products $[M + H]^{2+\bullet}$ and $[M + H]^{3+\bullet\bullet}$, respectively. The map also indicates that the m/z 1364.83 ion correlates negatively (blue features) with the Melittin precursor ions at m/z 1424.24 and also with the m/z 949.33, 934.75, 761.64, and 701.00 ions, which in turn correlates positively to the Melittin precursor at m/z 1424.24. These ions are then assigned to photoionization product ions of Melittin (see Figure 2). This grouping of the signals in two main groups is consistent with the anticorrelation observed between the two precursors in Figure S1. Since both ions contribute to the TIC, an increase in one ion's intensity results in a relative decrease in the other. All product ions from W8-Substance P are anticorrelated with those of Melittin, and vice versa. Additionally, all the fragment ions of a specific precursor are correlated with that precursor. The precursor of each product ion can then be immediately identified from the map.

In order to facilitate the analysis of the partial correlation map, hierarchical clustering calculations were performed. The idea is to group each ionic signal with the ones that share similarities with it. The dendrogram obtained is presented in Figure S2. To determine the optimal number of clusters, we applied the elbow method to the intracluster squared sum (WSS) and got four main clusters. The mass spectra corresponding to each cluster are presented in Figure 4 and compared to experimental photon activation mass spectra at 16 eV measured for each individual precursor alone.

Figure 4a compares the tandem mass spectrum of Cluster 1 and the experimental spectrum of W8-Substance P showing that all of the features of the experimental spectrum are also found on the cluster spectrum. The same is also observed in Figure 4c for Melittin and its clustering counterpart. Clusters 2 and 4 contain weak signals that appear to correspond to low-abundance fragments from W8-Substance P and Melittin, respectively. The agreement between the statistical data and the experimental measurements is excellent, showing the potential of statistical reconstruction of tandem mass spectra embedding two precursors.

https://doi.org/10.1021/jasms.5c00358
J. Am. Soc. Mass Spectrom. 2026, 37, 649−656

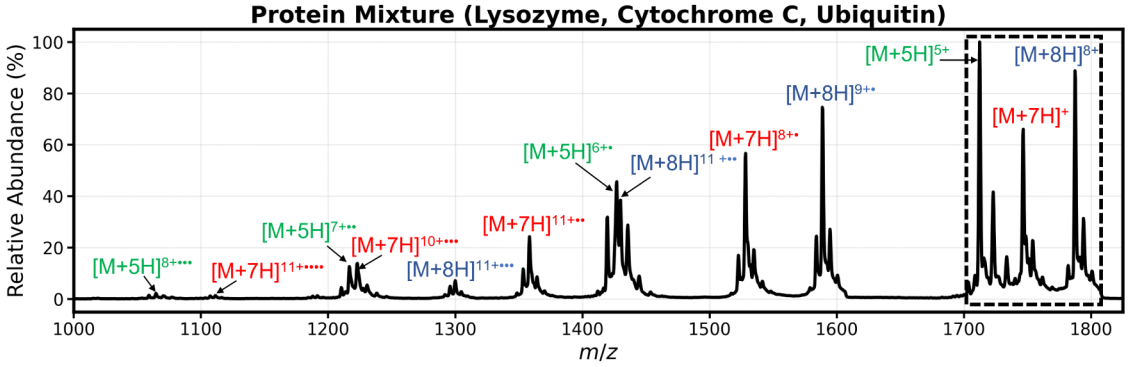

Figure 5. Average photon activation mass spectrum of simultaneous activation of the $[M+7H]^{7+}$ Cytochrome C ion (red labels), the $[M+5H]^{5+}$ Ubiquitin ion (green labels), and the lysozyme $[M+8H]^{8+}$ ion (blue labels) at 20 eV and 500 ms irradiation. The dotted box indicates the m/z selection region.

Three-Precursor Mixture

A more complex experiment involved the simultaneous photoactivation (20 eV, 500 ms) of three protein ions, from lysozyme, Cytochrome C, and Ubiquitin, centered around m/z 1760 with a 100 Th selection width. Approximately 800 mass spectra were acquired. Figure 5 presents the resulting average tandem mass spectrum. The green labels in Figure 5 refer to Ubiquitin ions, the red labels to Cytochrome C ions, and the blue labels to lysozyme ions.

The ionization energies of Cytochrome C and Ubiquitin have been reported previously.[26] The $[M+7H]^{7+}$ (m/z 1746.67) Cytochrome C ion and the $[M+5H]^{5+}$ (m/z 1712.33) ion of Ubiquitin have been found to have an ionization energy close to 13 eV. Although the ionization energy of the $[M+8H]^{8+}$ (m/z 1787.33) lysozyme ion has not been reported, it is expected to be similar in magnitude owing to its comparable size and charge state. Given the relatively long irradiation time, radical cations produced by the precursor photoionization could absorb additional photons, leading to further ionization. This mechanism results in consecutive multiple photoionization events, as previously described for peptides (Table 1).

Table 1. Precursors and Main Photoproducts Observed from the Simultaneous Activation of the $[M+7H]^{7+}$ Cytochrome C Ion, the $[M+5H]^{5+}$ Ubiquitin Ion, and the Lysozyme $[M+8H]^{8+}$ Ion at 20 eV and 500 ms Irradiation

Protein	Species	m/z (Exp.)	Charge (z)	Relative abundance (%)
Lysozyme	$[M+8H]^{8+}$	1787.33	8	97.32
	$[M+8H]^{9+\bullet}$	1588.67	9	81.65
	$[M+8H]^{10+\bullet\bullet}$	1430.00	10	40.65
	$[M+8H]^{11+\bullet\bullet\bullet}$	1300.00	11	7.66
Cytochrome C	$[M+7H]^{7+}$	1746.67	7	70.38
	$[M+7H]^{8+\bullet}$	1528.33	8	60.44
	$[M+7H]^{9+\bullet\bullet}$	1358.33	9	25.71
	$[M+7H]^{10+\bullet\bullet\bullet}$	1222.67	10	13.94
	$[M+7H]^{11+\bullet\bullet\bullet\bullet}$	1111.33	11	1.42
Ubiquitin	$[M+5H]^{5+}$	1712.33	5	100
	$[M+5H]^{6+\bullet}$	1427.00	6	45.90
	$[M+5H]^{7+\bullet\bullet}$	1223.00	7	14.14
	$[M+5H]^{8+\bullet\bullet\bullet}$	1070.33	8	1.23

Similarly to the two precursor cases, a 1% relative abundance threshold was applied to the data. For this three-precursor mixture, conditional mutual information (CMI) was used instead of correlation analysis. Indeed, the relative abundances of the precursor ions (Figure S3) indicated that a simple correlated/anticorrelated separation was no longer appropriate. CMI, a metric commonly used to measure the degree of similarity between variables, was used. Unlike correlation, CMI can detect any type of relationship, whether linear or not, and is null in the absence of a relationship, with a positive value indicating the strength of that relationship. CMI is the information theoric counterpart of partial correlation and is expressed as

$$I(X;\ Y|Z) = \sum_{x\in X}\sum_{y\in Y}\sum_{z\in Z} p(x,\ y,\ z)\log\left(\frac{p(x,\ y|z)}{p(x|z)p(y|z)}\right) \quad (2)$$

where X and Y are the signals of interest and Z is the condition variable. The CMI map is presented in Figure 6. The diagonal representing the self-relationship of the variable has been removed for clarity. The relationship between ions is obvious: each precursor ion aligns vertically and horizontally with its products, as indicated on the figure by the dotted colored lines. The color scheme from Figure 5 is retained.

Hierarchical clustering was again applied, and the mass spectra corresponding to each of the four identified clusters were calculated. The reconstructed spectra are compared to the experimental ones for the individual precursors in Figure 7. The agreement is excellent, as the reconstructed tandem mass spectra match perfectly the experimental spectra for lysozyme (panel a), Ubiquitin (panel c), and Cytochrome C (panel d). Cluster 2 (Figure 7b) corresponds to noise and low-abundance signals that could not be assigned to the main precursor ion family. Notably, the region around m/z 1428 contains Ubiquitin $[M+5H]^{6+\bullet}$ at m/z 1427 and lysozyme $[M+8H]^{10+\bullet\bullet}$ at m/z 1430. Figure 5 shows that the two signals are nearly superimposed, resulting in a complex feature around m/z 1428. The clustering approach successfully resolved this composite feature, correctly assigning signals to their respective precursors (Figure 7a and c).

In addition, the region around m/z 1222 also contains a mixture of the Cytochrome $[M+7H]^{10+\bullet\bullet\bullet}$ ion (m/z 1222.67) and the Ubiquitin $[M+5H]^{7+\bullet\bullet}$ ion (m/z 1223). Most of the signal is assigned to Ubiquitin (Cluster 3, Figure 7c), with only a small part assigned to Cytochrome C (Cluster 4, Figure 7d).

https://doi.org/10.1021/jasms.5c00358
J. Am. Soc. Mass Spectrom. 2026, 37, 649−656

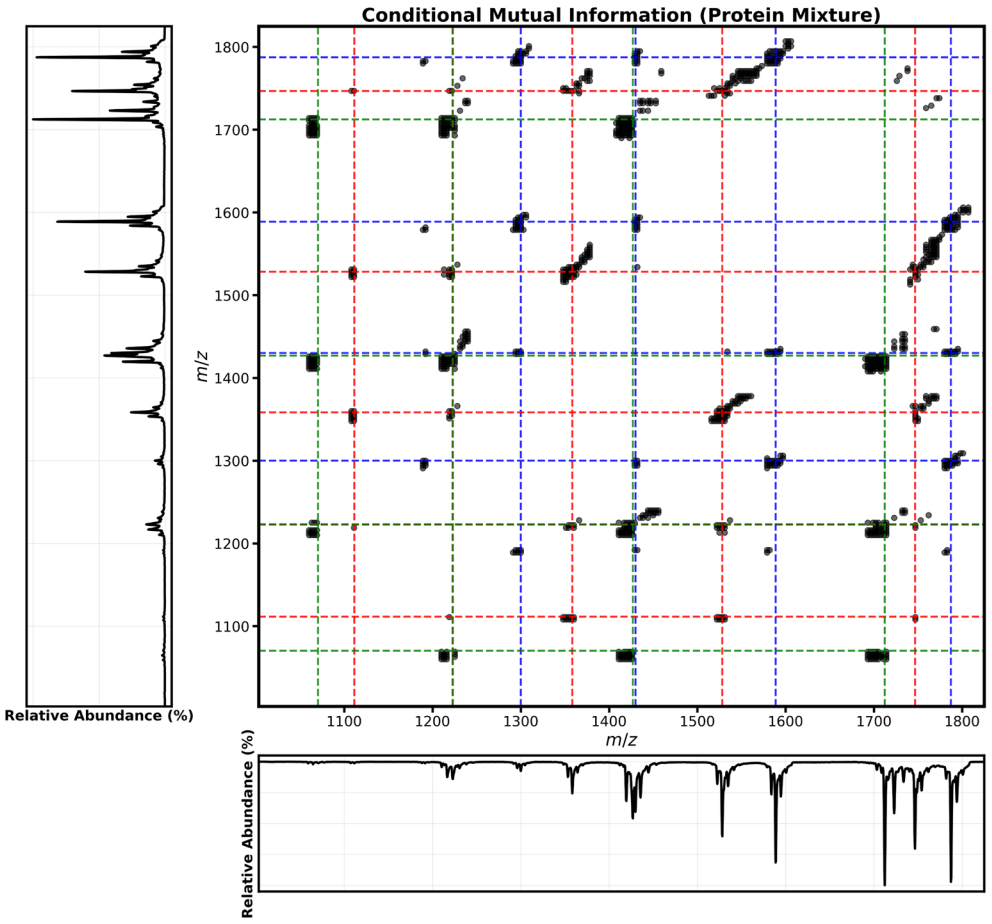

Figure 6. Average photon activation mass spectrum of a mixture of cytochrome C, lysozyme, and Ubiquitin at 20 eV and 500 ms irradiation. The dotted lines indicate the groups to which each signal belongs with blue color for lysozyme, red for Cytochrome C, and green for Ubiquitin.

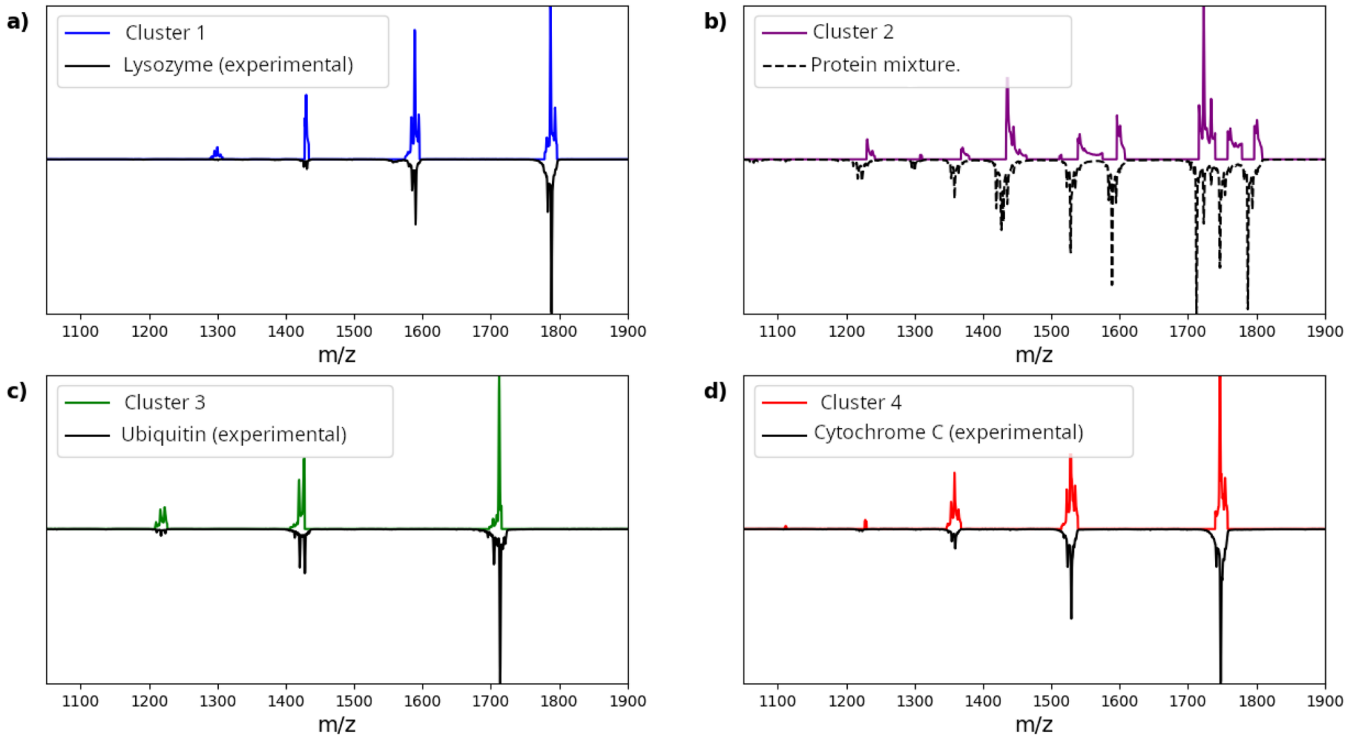

Figure 7. Comparison of reconstructed tandem mass spectra for each cluster with experimental spectra for lysozyme (a), Ubiquitin (c), and Cytochrome C (d). Cluster 2 (b) represents noise and unassigned ions.

https://doi.org/10.1021/jasms.5c00358
J. Am. Soc. Mass Spectrom. 2026, 37, 649−656

Even in congested regions, CMI effectively identified the origin of the product ions.

CONCLUSION

This work reports the application of correlation and information-theoretic treatments combined with clustering analysis to tandem mass spectra of a mixture of precursors activated simultaneously to resolve MS/MS spectra of individual precursors. Partial correlation analysis provides an intuitive visualization of complementary and anticorrelated fragments but requires careful interpretation of the signs. In contrast, conditional mutual information (CMI) analysis captures the nonlinear dependencies and yields a positive metric, which is easily interpretable. The two methods are complementary to covariance mapping. Both partial correlation and CMI analyses in combination with clustering analysis reveal precursor-specific fragment relationships, enabling the reconstruction of individual spectra from chimeric data without prior knowledge of the mixture of precursors. The approach is validated on both two- and three-protein mixtures. We plan to apply this approach in ion action spectroscopy, which requires precise knowledge of the precursor and product abundances to derive the fragmentation yields as a function of the photon wavelength.[3] Moreover, the ability to identify the origin of fragments and potentially assess consecutive multiple fragmentation could help to guide the selection of experimental conditions, such as irradiation time, photon wavelength, or photon source flux. Beyond photon activation, the proposed data-driven framework, which combines statistical and clustering analysis, can be applied to other activation techniques where simultaneous fragmentation of multiple precursors occurs.

ASSOCIATED CONTENT

Supporting Information

The Supporting Information is available free of charge at https://pubs.acs.org/doi/10.1021/jasms.5c00358.

Data and code availability, total ion chromatograms, and clustering data (PDF)

AUTHOR INFORMATION

Corresponding Author

Alexandre Giuliani − *Synchrotron SOLEIL, L'Orme des Merisiers, Saint Aubin, Gif-sur-Yvette 91192, France; Transform Department, UAR1008, INRA, Nantes 44316, France;* orcid.org/0000-0003-1710-4933; Email: alexandre.giuliani@synchrotron-soleil.fr

Authors

Félix Truong − *Synchrotron SOLEIL, L'Orme des Merisiers, Saint Aubin, Gif-sur-Yvette 91192, France;* Present Address: LIST/UAF, CEA Saclay, 91191 Gif-sur-Yvette, France

Laurent Nahon − *Synchrotron SOLEIL, L'Orme des Merisiers, Saint Aubin, Gif-sur-Yvette 91192, France;* orcid.org/0000-0001-9898-5693

Complete contact information is available at: https://pubs.acs.org/10.1021/jasms.5c00358

Author Contributions

The manuscript was written through contributions of all authors. All authors have given approval to the final version of the manuscript.

Funding

INRAE and SOLEIL doctoral thesis grant.

Notes

The authors declare no competing financial interest.

ACKNOWLEDGMENTS

F.T. thanks INRAE and Synchrotron SOLEIL for a joint doctoral fellowship grant. We are grateful to the general staff of SOLEIL for running the facility smoothly and providing synchrotron radiation beamtime under proposals 20230353 and 20240517. We would like to thank J.-F. Gil for his technical assistance in using the DESIRS beamline.

REFERENCES

(1) Reilly, J. P. Ultraviolet Photofragmentation of Biomolecular Ions. *Mass Spectrom. Rev.* **2009**, *28*, 425−447.

(2) Brodbelt, J. S.; Morrison, L. J.; Santos, I. Ultraviolet Photodissociation Mass Spectrometry for Analysis of Biological Molecules. *Chem. Rev.* **2020**, *120*, 3328−3380.

(3) Antoine, R.; Dugourd, P. UV-Visible Absorption Spectroscopy of Protein Ions. In *Photophysics of Ionic Biochromophores. Physical Chemistry in Action*; Brøndsted Nielsen, S.; Wyer, J., Eds.; Springer: Berlin, Heidelberg, 2013, pp 141−153. DOI: 10.1007/978-3-642-40190-9_8.

(4) Giuliani, A.; Williams, J. P.; Green, M. R. Extreme Ultraviolet (XUV) Radiation: A Means of Ion Activation for Tandem Mass Spectrometry. *Anal. Chem.* **2018**, *90*, 7176−7180.

(5) Ickert, S.; Beck, S.; Linscheid, M. W.; Riedel, J. VUV Photodissociation Induced by a Deuterium Lamp in an Ion Trap. *J. Am. Soc. Mass Spectrom.* **2019**, *30*, 2114−2122.

(6) Giuliani, A.; Milosavljević, A. R.; Canon, F.; Nahon, L. Contribution of Synchrotron Radiation to Photoactivation Studies of Biomolecular Ions in the Gas Phase. *Mass Spectrom. Rev.* **2014**, *33*, 424−441.

(7) Bari, S.; Gonzalez-Magaña, O.; Reitsma, G.; Werner, J.; Schippers, S.; Hoekstra, R.; Schlathölter, T. Photodissociation of Protonated Leucine-Enkephalin in the VUV Range of 8−40 eV. *J. Chem. Phys.* **2011**, *134*, 024314−024314.

(8) Milosavljević, A. R.; Canon, F.; Nicolas, C.; Miron, C.; Nahon, L.; Giuliani, A. Gas-Phase Protein Inner-Shell Spectroscopy by Coupling an Ion Trap with a Soft X-ray Beamline. *J. Phys. Chem. Lett.* **2012**, *3*, 1191−1196.

(9) Frasinski, L. J.; Codling, K.; Hatherly, P. A. Covariance Mapping: A Correlation Method Applied to Multiphoton Multiple Ionization. *Science* **1989**, *246*, 1029−1031.

(10) Frasinski, L. J. Covariance Mapping Techniques. *J. Phys. B: At., Mol. Opt. Phys.* **2016**, *49*, 152004.

(11) Driver, T.; Cooper, B.; Ayers, R.; Pipkorn, R.; Patchkovskii, S.; Averbukh, V.; Klug, D. R.; Marangos, J. P.; Frasinski, L. J.; Edelson-Averbukh, M. Two-Dimensional Partial-Covariance Mass Spectrometry of Large Molecules Based on Fragment Correlations. *Phys. Rev. X* **2020**, *10*, 041004.

(12) Driver, T.; Averbukh, V.; Frasiński, L. J.; Marangos, J. P.; Edelson-Averbukh, M. Two-Dimensional Partial Covariance Mass Spectrometry for the Top-Down Analysis of Intact Proteins. *Anal. Chem.* **2021**, *93*, 10779−10788.

(13) Driver, T.; Pipkorn, R.; Averbukh, V.; Frasinski, L. J.; Marangos, J. P.; Edelson-Averbukh, M. Identification of Cofragmented Combinatorial Peptide Isomers by Two-Dimensional Partial Covariance Mass Spectrometry. *J. Am. Soc. Mass Spectrom.* **2023**, *34*, 1230−1234.

(14) Lee, J. C.; özer, B. R.; Heo, I.; Schultz, T. Correlating Parent-Fragment Relationships in Cluster Photoionization. *arXiv* 2402.08398, **2024**.
(15) Servant, F.; Nahon, L.; Giuliani, A.. *Procédé de reconstruction d'un spectre de masse* , FR3149423A1, 2023.
(16) Li, Y.; Cavet, G.; Zare, R. N.; Driver, T. Fragment Correlation Mass Spectrometry: Determining the Structures of Biopolymers in a Complex Mixture without Isolating Individual Components. *Proc. Natl. Acad. Sci. U. S. A.* **2024**, *121*, No. e2409676121.
(17) Milosavljević, A. R.; Nicolas, C.; Gil, J.-F. F.; Canon, F.; Réfrégiers, M.; Nahon, L.; Giuliani, A. VUV Synchrotron Radiation: A New Activation Technique for Tandem Mass Spectrometry. *J. Synchrotron Radiat.* **2012**, *19*, 174−178.
(18) Nahon, L.; De Oliveira, N.; Garcia, G.; Gil, J. F.; Pilette, B.; Marcouillé, O.; Lagarde, B.; Polack, F. DESIRS: A State-of-the-Art VUV Beamline Featuring High Resolution and Variable Polarization for Spectroscopy and Dichroism at SOLEIL. *J. Synchrotron Radiat.* **2012**, *19*, 508−520.
(19) Bezanson, J.; Karpinski, S.; Shah, V. B.; Edelman, A. Julia: A Fast Dynamic Language for Technical Computing. *arXiv* 1209.5145, **2012**.
(20) Giuliani, A. *Mass J: Julia Package for Mass Spectrometry Data Treatment and Analysis, version V1, 2021*; Data INRAE, DOI: 10.15454/KU1P28.
(21) Truong, F.; Giuliani, A. *Entropy-Invariant*, 2025. https://github.com/Entropy-Invariant/EntropyInvariant.jl.
(22) Xiong, H.; Li, Z.. *Data Clustering Algorithms and Applications*; CRC Press. 2014.
(23) Canon, F.; Milosavljević, A. R.; Nahon, L.; Giuliani, A. Action Spectroscopy of a Protonated Peptide in the Ultraviolet Range. *Phys. Chem. Chem. Phys.* **2015**, *17*, 25725−25733.
(24) Budnik, B. A.; Tsybin, Y. O.; Häkansson, P.; Zubarev, R. A. Ionization Energies of Multiply Protonated Polypeptides Obtained by Tandem Ionization in Fourier Transform Mass Spectrometers. *J. Mass Spectrom.* **2002**, *37*, 1141−1144.
(25) Budnik, B. A.; Zubarev, R. A. $MH^{2+\bullet}$ Ion Production from Protonated Polypeptides by Electron Impact: Observation and Determination of Ionization Energies and a Cross-Section. *Chem. Phys. Lett.* **2000**, *316*, 19−23.
(26) Giuliani, A.; Milosavljević, A. R.; Hinsen, K.; Canon, F.; Nicolas, C.; Réfrégiers, M.; Nahon, L. Structure and Charge-State Dependence of the Gas-Phase Ionization Energy of Proteins. *Angew. Chem. Int. Ed.* **2012**, *51*, 9552−9556.

https://doi.org/10.1021/jasms.5c00358
J. Am. Soc. Mass Spectrom. 2026, 37, 649−656